高等学校化学学报
CHEMICAL JOURNAL OF CHINESE UNIVERSITIES
研究论文

蒙脱石负载氧化铈纳米酶用于克罗恩肠炎治疗

陈夕雯[1#]，程超群[1#]，程　远[1#]，赵　升[1]，魏　辉[1,2]
（1. 南京大学现代工程与应用科学学院，生物医学工程系，南京固体微结构国家实验室，
江苏省人工功能材料重点实验室，南京 210023；
2. 南京大学化学化工学院，化学与生物医药创新研究院，
生命科学分析化学国家重点实验室和配位化学国家重点实验室，南京 210023）

摘要　通过水热法合成由临床用药蒙脱石(Montmorillonite, MMT)负载的高效纳米酶氧化铈(Cerium dioxide, CeO_2)，通过开展体内外实验，拓展其在炎症性肠病治疗中的普适性. 结果显示，CeO_2@MMT具有良好的类超氧化物歧化酶活性及类过氧化氢酶活性，并且在小鼠克罗恩病的治疗中体现了明显的疗效及优异的生物安全性，为CeO_2@MMT的应用拓宽了方向.

关键词　炎症性肠病；克罗恩病；氧化铈基纳米酶；蒙脱石；活性氧物种
中图分类号　O643；R318　　**文献标志码**　A　　doi：10.7503/cjcu20220476

CeO_2@montmorillonite Nanozyme for Crohn's Disease Therapy

CHEN Xiwen[1#], CHENG Chaoqun[1#], CHENG Yuan[1#], ZHAO Sheng[1], WEI Hui[1,2*]
(*1. Department of Biomedical Engineering, College of Engineering and Applied Sciences, Nanjing National Laboratory of Microstructures, Jiangsu Key Laboratory of Artificial Functional Materials, Nanjing* 210023;
2. State Key Laboratory of Analytical Chemistry for Life Science and State Key Laboratory of Coordination Chemistry, Chemistry and Biomedicine Innovation Center (ChemBIC), School of Chemistry and Chemical Engineering, Nanjing University, Nanjing 210023, *China*)

Abstract　Inflammatory bowel disease (IBD) is a chronic, nonspecific disease that is refractory and therefore affects the normal life of patients to a great extent. Although the global incidence of this disease is increasing year by year, ideal therapeutic drugs are still lacking in clinical practice. Inspired by the antioxidant activity of natural enzymes in organisms, the therapeutic strategies of natural enzymes for inflammatory diseases have come into view. However, natural enzymes have the limitations of poor stability and high cost. Here, we loaded cerium oxide on a montmorillonite surface to obtain CeO_2@montmorillonite (CeO_2@MMT) nanozyme and verified that it has an excellent curative effect and universality in the treatment of Crohn's disease (CD) through *in vitro* and *in vivo* experiments. CeO_2@MMT

收稿日期：2022-04-11. 网络首发日期：2022-08-24.
联系人简介：魏　辉，男，博士，教授，主要从事生物纳米功能材料、生物纳米医学及体外诊断与个体化诊疗方面的研究.
E-mail: weihui@nju.edu.cn
基金项目：国家重点研究发展计划项目(批准号：2019YFA0709200，2021YFF1200700)、国家自然科学基金(批准号：21874067)、中国科学院跨学科创新团队(批准号：JCTD-2020-08)、江苏高校优势学科建设工程资助项目(PAPD)、南京大学创新基金和中央高校基础研究基金(批准号：021314380195)资助.
Supported by the the National Key Research and Development Program of China(Nos. 2019YFA0709200, 2021YFF1200700), the National Natural Science Foundation of China(No. 21874067), the CAS Interdisciplinary Innovation Team(No. JCTD-2020-08), the Priority Academic Program Development of Jiangsu Higher Education Institutions(PAPD Program), China, the Innovation Foundation of Nanjing University, China and the Fundamental Research Funds for the Central Universities, China(No.021314380195).
共同第一作者.

showed good superoxide dismutase- and catalase-like activity *in vitro*. Its negative charges enable it to target the positively charged intestinal inflammatory site and exert an anti-inflammatory effect at the focus. Thus, it showed obvious curative effects and excellent biosafety in the treatment of CD in mice, which broadened the spectrum of the application of nanozymes.

Keywords Inflammatory bowel disease; Crohn's disease; Cerium oxide-based nanozyme; Montmorillonite; Reactive oxygen species

1 Introduction

Inflammatory bowel disease (IBD), including ulcerative colitis (UC) and Crohn's disease (CD), is a chronic nonspecific inflammatory disease with still unclear etiology as well as gastrointestinal involvement[1,2]. In the past few decades, the incidence of IBD in western countries was significantly higher than that in Asian countries. In 2015, the incidence of IBD in western countries was about 0.5%. In recent years, with the continuous development of newly industrialized Asian countries, the incidence of IBD in Asian countries has also been increasing yearly[3]. Compared with other malignant diseases, although the direct fatality rate of IBD is not high, the pain and inconvenience caused by the illness seriously affect the life quality of patients. In addition, if there is a serious lesion in the intestinal inflammatory site, it may further develop into malignant diseases such as colon cancer (individuals with IBD have a 2—3 times higher risk of developing colorectal cancer than those who do not)[4].

At present, drugs such as 5-aminosalicylic acid (5-ASA), hormones and immunosuppressants are usually used to treat IBD clinically[5]. 5-ASA is mainly effective for mild to moderate IBD patients, but sometimes it may bring side effects such as allergic reaction, jaundice and abdominal pain. Hormone drugs have better therapeutic efficacy than 5-ASA, but they have side effects that cannot be ignored (such as an increased risk of infection, osteoporosis and impaired glucose tolerance). Therefore, hormone drugs are mainly used to induce remission of moderate to severe IBD patients but not for long-term maintenance therapy. Immunosuppressants are also limited by their side effects (such as myelosuppression), thus, it is difficult to be widely used in clinical practice. In addition, taking characteristics of IBD into consideration, such as a chronic course, easy recurrence, and difficult recovery, patients usually need to take medicine for a long time, which is more likely to cause various complications, such as antibiotic resistance and immune response[6]. To address the above clinical need, many researchers have developed targeted therapy systems for treating IBD to reduce the drug dose, increase the local drug concentration, and inhibit the side effects of drugs[7—10]. However, to date, the therapeutics that can target specific lesions of IBD have not been fully developed.

The pathogenic site of IBD is characterized by an increase in reactive oxygen species (ROS)[11,12]. Excessive ROS destroys the redox homeostasis of cells, thus causing damage to cells and tissues, which plays an important role in the onset and development of IBD[11]. Inspired by an organism's self-regulation ability towards oxidative stress, researchers have used natural enzymes with ROS scavenging ability, such as superoxide dismutase (SOD) and catalase (CAT), to regulate excessive ROS caused by pathological changes and maintain normal physiological function[13]. However, natural enzymes have the intrinsic disadvantages of poor stability, high cost, and immunogenicity, which hinder their further application[14]. Therefore, it is of great importance to use abiological materials to mimic enzymes. Among them, the functional nanomaterials with enzyme-like activities (called nanozymes) have shown great promise in disease therapy[15—19].

Inspired by the characteristic that the pathogenic site of IBD is rich in positively charged proteins[10], we have designed CeO_2@MMT nanozyme, which is a combination of montmorillonite (MMT, a natural clinical drug with negative charges) and cerium oxide nanoparticles, for targeting inflammatory sites. The

CeO_2@MMT nanozyme showed an excellent ROS scavenging effect *in vitro* and good therapeutic efficacy for UC mouse model in our previous study[20].

Nevertheless, the therapeutic effects of nanozymes towards CD, the other type of IBD, have been much less studied. To fill this gap and to verify its universality in the treatment of IBD, herein we studied the therapeutic efficacy of CeO_2@MMT nanozyme towards CD (Fig. 1). We intentionally used commercial MMT powder from pharmacy instead of the pure MMT reagent used in our previous research to prepare the CeO_2@MMT nanozyme[20]. After removing the excipient materials from commercial MMT, the obtained MMT was used to synthesize CeO_2@MMT. It was verified by various characterization methods that CeO_2 successfully grew on the surface of MMT, and CeO_2@MMT had excellent enzymatic activities *in vitro*. Furthermore, compared with 5-ASA, we proved that CeO_2@MMT, which could be adsorbed on the colon lesion, can eliminate redundant ROS, thus reducing the inflammation of the lesion, promoting an anti-inflammatory immune response, and finally effectively treating 2,4,6-trinitrobenzene sulfonic acid sol (TNBS)-induced CD in a murine model.

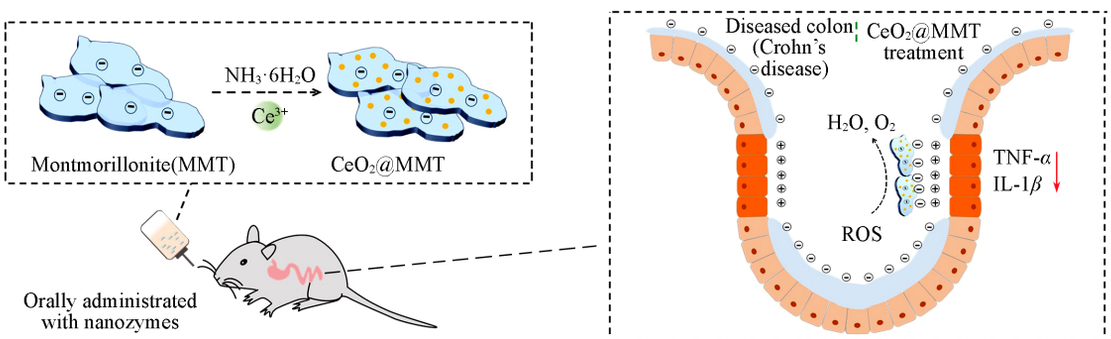

Fig. 1 Design and synthesis of CeO_2@MMT nanozyme for the treatment of inflammatory bowel disease(IBD)

2 Experimental

2.1 Materials

Cerium nitrate hexahydrate (99.95%), ethylene glycol (analytically pure, 98%), and concentrated ammonia solution (analytically pure, 25%—28%) were purchased from Shanghai Aladdin Biochemical Technology Co., Ltd. Montmorillonite powder (MMT) was purchased from Hangzhou Kangenbei Pharmaceutical Co., Ltd., and the approval number is Sinopharm Zhunzi H20074198. All other analytical pure reagents and chemicals were purchased from commercial companies and used according to regulations without pretreatment. The experimental water was prepared by a Millipore Milli-Q water purification system (Billica Company, USA).

2.2 Material Characterizations

Material size, morphology, structure and element distribution information were obtained by an FEI TECNAI F20 transmission electron microscope (TEM, FEI, Netherlands, accelerating voltage 200 kV) and a Quanta 200 scanning electron microscope (SEM, FEI, Netherlands, accelerating voltage 10 kV). X-ray diffraction (XRD) pattern were obtained by a Rigaku Ultima powder diffractometer (Rigaku, Japan, excitation source: Cu *Kα*). The working voltage was 40 kV, the current was 40 mA, and the scanning rate was 2°/min. X-ray photoelectron spectroscopy (XPS) was performed by using a Thermo Scientific *Kα* spectrometer (Thermo Fisher, USA). The *zeta* potential (25 ℃) of the sample was detected by a Malvin Zetasizer NanoZSP (Malvin, UK). An inductively coupled plasma emission spectrometer (ICP-OES, PerkinElmer's Avio®500, PerkinElmer, USA) was used to quantify the concentration of cerium oxide in all samples.

2.3 Synthesis of CeO_2 and CeO_2@MMT

Preparation of ethylene glycol solution of $Ce(NO_3)_3 \cdot 6H_2O$ and MMT suspension: 126 mg of $Ce(NO_3)_3 \cdot 6H_2O$ crystal was added to 10 mL of ethylene glycol to obtain an ethylene glycol solution of $Ce(NO_3)_3 \cdot 6H_2O$. 5 g of purified MMT powder was added to 100 mL of water and stirred vigorously for 48 h to form a uniformly dispersed MMT suspension with a concentration of 50 mg/mL.

As the purchased MMT powder consists of MMT and other auxiliary materials, to obtain pure MMT, the purchased MMT powder was dispersed in water, stirred vigorously for 24 h, and then centrifuged several times to remove other auxiliary materials, such as glucose. The purified MMT was used to prepare the above MMT suspension.

Preparation of the mixed solution: 10 mL of ethylene glycol solution of $Ce(NO_3)_3 \cdot 6H_2O$ was dropped into the prepared 10 mL-MMT suspension and stirred vigorously for more than 5 min. Then, the above mixed solution was placed into a water bath at 60 ℃ and stirred vigorously for 10 min.

Hydrothermal synthesis: 1.6 mL of concentrated ammonia solution (28%—30%) was quickly injected into the mixed solution with a syringe. The mixed solution was stirred vigorously in a 60 ℃ water bath, and after 3 h, the synthesized CeO_2@MMT was collected by centrifugation. Centrifugation and washing with water were repeated until the pH of the supernatant solution became neutral.

The CeO_2@MMT product was re-dispersed in water or lyophilized for later use.

Using the same synthesis method, cerium oxide nanoparticles were prepared without adding MMT and labeled as CeO_2.

2.4 SOD-like Activity Measurements

The SOD activity of CeO_2, MMT, and CeO_2@MMT was detected by using a SOD kit (Dojindo, Japan). First, 20 μL of each group of samples containing cerium oxide (the final concentrations of cerium oxide were 12.5, 25 and 50 μg/mL, respectively) was mixed with 200 μL of water-soluble tetrazolium salt, 2-(4-iodophenyl)-3-(4-nitrophenyl)-5-(2,4-disulfophenyl)(WST-1). Then, the absorbance at 450 nm was detected by a multi-functional microplate reader (Tecan Infinite 200 Pro). The $^{\cdot}O_2^-$ clearance rate of each group of samples was calculated by the measured absorbance change value.

2.5 Catalase-like Activity Measurements

The catalase-like (CAT) activities of CeO_2, MMT and CeO_2@MMT were evaluated by detecting the dissolved oxygen (dissolved O_2) content in the hydrogen peroxide reaction system added to the sample. Each group of samples was mixed with H_2O_2 to prepare a 6 mL-reaction system, and the final concentration of H_2O_2 was 5 mmol/L. At room temperature, the change of dissolved oxygen (mg/L) in the reaction system within 10 min after adding samples was detected by a SevenExcellence Multiparameter every 30 s.

2.6 Cell Culture, Cytotoxicity and Intracellular ROS Scavenging Capacity of Materials

RAW264.7 cells were acquired from the cell bank of the Chinese Academy of Sciences (Shanghai, China). Cells were cultured in high glucose-DMEM medium (Gibco, USA) containing 5% or 10% (volume ratio) FBS and 1% penicillin/streptomycin in a humidified 5% CO_2 atmosphere at 37 ℃.

Cytotoxicity: RAW264.7 cells were seeded at 8×10^3 cells per well in 96-well plates. After 1 d, different concentrations of materials were added to the cells. Cell viability (%) was quantified after 24 h of incubation using CCK-8 (Dojindo Laboratories, Japan) according to the manufacturer's instructions by a microplate reader (Tecan Infinite 200 Pro).

$$\text{Cell viability}=(A_t-A_b)/(A_c-A_b)\times100\%$$

where, A_t is the absorbance of the test samples, A_b is the absorbance of the blank groups (with no cells), and A_c is the absorbance of the control groups.

ROS scavenging ability of RAW264.7 cells: RAW264.7 cells were seeded at 8×10^3 cells per well in 96-well plates. After 1 d, refreshed growth medium containing different concentrations of materials was added and further incubated for 2 h. Next, H_2O_2 was added to each well to stimulate all groups (final concentration is 100 μmol/L) for 30 min except for the negative control group. After stimulation, the cells were incubated with 2′,7′-dichlorofluorescin diacetate (DCFH-DA, Shanghai Aladdin Biochemical Technology) for 20 min, washed with phosphate buffer solution (PBS) three times, and analyzed by using a multiple plate reader (Tecan Infinite 200 Pro). The excitation wavelength was 488 nm.

2.7 *In vivo* Anti-inflammation Therapies

All the animal studies were approved by the Committee for Experimental Animals Welfare and Ethics of Nanjing University (Approval number: IACUC-2107009).

The Crohn's disease (CD) model of mice was chosen and established with 2,4,6-trinitrobenzene sulfonic acid (TNBS)-induced colitis to evaluate the antiinflammation of nanozyme. Male C57BL/6 mice (18 to 20 g) were acclimatized for 7 d and randomly divided into various groups with five mice per group (n=5). The TNBS induced mice were pre-sensitized with 1% (mass fraction) TNBS, kept for 7 d, and treated with mass fraction of 2.5% TNBS enema on Day 8. CeO_2 NPs, MMT, CeO_2@MMT, and 5ASA were orally administered once per day on three consecutive days (Days 9, 10, and 11). The mice of all groups were sacrificed after anesthetization with diethyl ether on Day 12. The body weight and length of the whole colon were recorded, respectively.

2.8 Pathological Evaluation and Cytokines Determination with ELISA Kits

The colon tissues from all groups were fixed with 10% formalin, processed routinely, dried and embedded into paraffin, sectioned at a thickness of 4 μm, and stained with hematoxylin and eosin (H&E). The stained tissues were examined and photographed by using an optical microscope.

For proinflammatory cytokines evaluation, the amounts of TNF-α and IL-1β in colon homogenate were quantified by enzyme-linked immunosorbent assay (ELISA) kits. The colon tissue with a length of about 5 mm from each mouse was weighed and homogenized in 1.5 mL of saline at 4 ℃. The resultant homogenate was centrifuged at 2000 r/min for 20 min at 4 ℃, and the supernatant was collected for evaluation. Commercial mouse IL-1β and TNF-α ELISA Kits (Neobioscience Technology Co. Ltd., China) were used to quantify the amounts of IL-1β and TNF-α in the homogenate of colon tissues, respectively.

3 Results and Discussion

3.1 Synthesis and Characterization of CeO_2@MMT

To show the translational promise of CeO_2@MMT, clinical grade MMT powder was used in the current study. Since clinical MMT powder has other excipient materials, these materials were removed to obtain pure MMT as follows. The MMT powder was dispersed in water, stirred vigorously for 24 h, and then centrifuged several times to obtain the MMT suspension. CeO_2@MMT was prepared *in situ* by mixing $Ce(NO_3)_3\cdot6H_2O$ ethylene glycol solution with the pre-treated MMT suspension in a volume ratio of 1∶1[20]. TEM images (Fig.2) show that CeO_2@MMT maintained a sheet structure similar to that of MMT, while CeO_2 nanoparticles (CeO_2 NPs) were uniformly loaded on the MMT sheets. Compared with free CeO_2 NPs (the particle size is about 5.5 nm), CeO_2 NPs loaded on MMT sheets (the particle size is about 3.9 nm) has better dispersibility and smaller size. In addition, SEM and energy dispersive spectroscopy (EDS) were used to image CeO_2@MMT at low magnification and analyze the composition. The energy spectra of Si, Al, O, and Ce elements in CeO_2@MMT were recorded. As shown in Fig. 3, the energy spectrum distribution diagram of Ce further confirmed that compared with free CeO_2 NPs, CeO_2 NPs loaded on MMT sheets had better dispersibility.

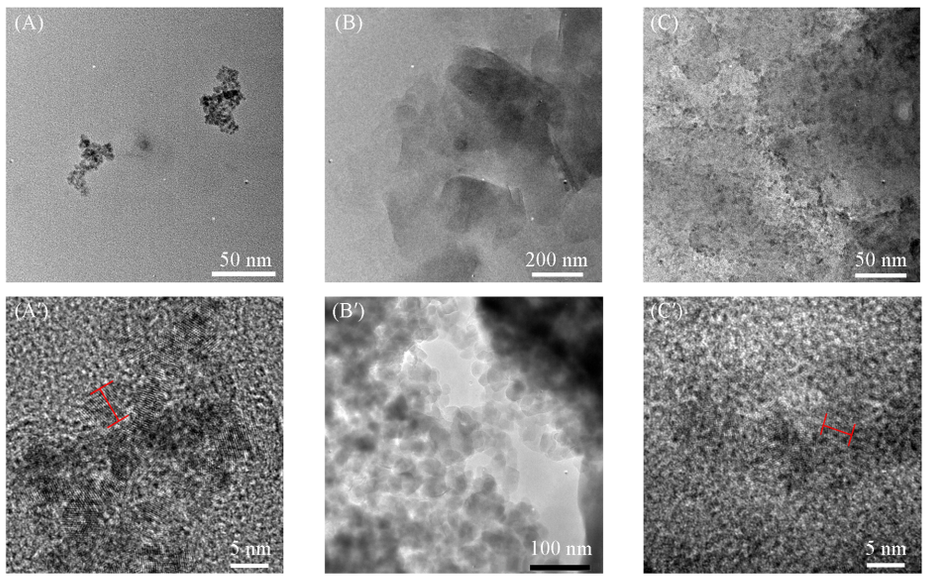

Fig. 2　TEM images of CeO_2(A, A′), MMT(B, B′) and CeO_2@MMT(C, C′) with different magnifIcations

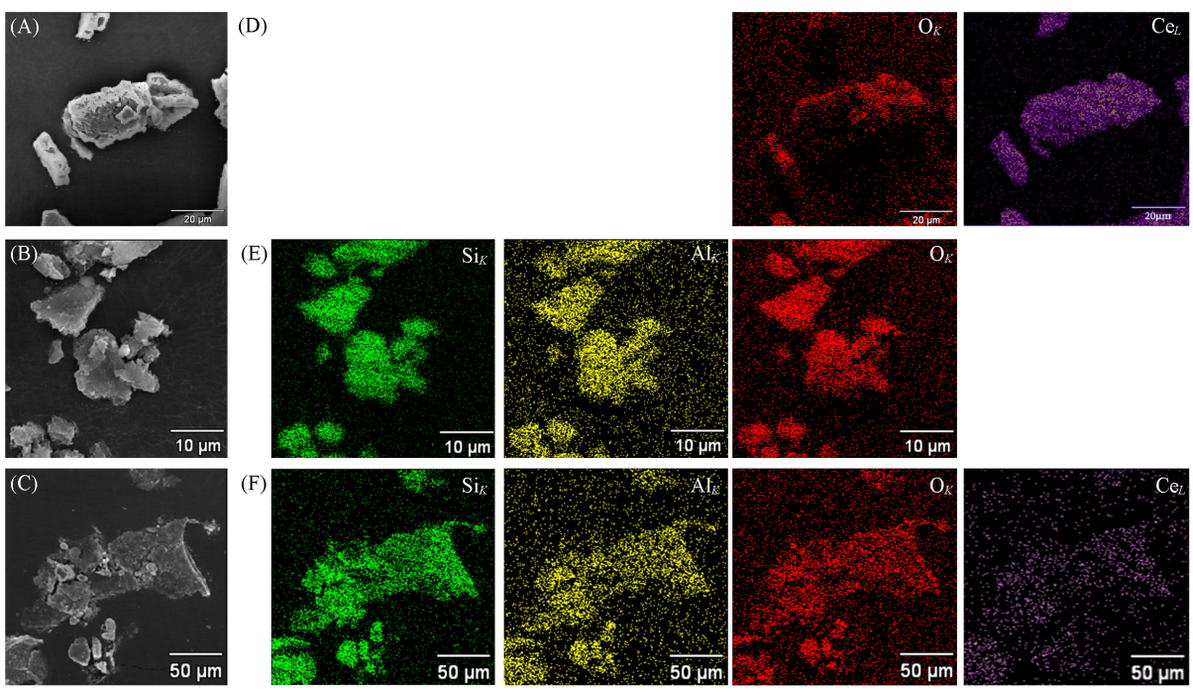

Fig. 3　SEM(A—C) and EDS(D—F) images of CeO_2(A, D), MMT(B, E), and CeO_2@MMT(C, F)

The crystalline characteristics of the materials were characterized by XRD. As shown in Fig. 4(A), characteristic peaks of CeO_2 and CeO_2@MMT could be observed at 2θ=28.5°, 56.8°, and 76.7°, which indicated that CeO_2 successfully grew on the MMT surface.

Then, to determine the ability of the materials to target the inflammatory sites enriched with positively charged proteins[19], the *zeta* potentials of CeO_2, MMT, and CeO_2@MMT were determined. As shown in Fig.4(B), the *zeta* potential of CeO_2 was 11.37 mV, while the *zeta* potentials of MMT and CeO_2@MMT were both negative(−22.5 mV and −22 mV, respectively). The above results ensured the ability of CeO_2@MMT to target positively charged inflammatory sites.

The enzyme-like activity of CeO_2 NPs depends on the Ce^{3+}/Ce^{4+} ratio on their surface[21—24]. Therefore,

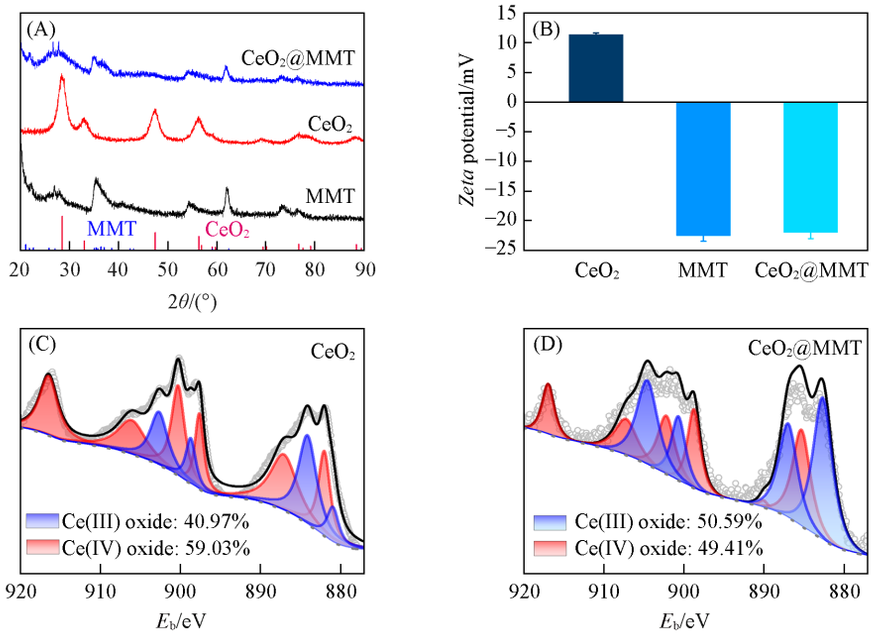

Fig. 4 XRD patterns(A), *zeta* potentials(B) and XPS spectra(C, D) of CeO_2, MMT and CeO_2@MMT

(B) Data are presented as mean±standard error of the mean(n=3).

X-ray photoelectron spectroscopy(XPS) was used to study the valence state and ratio of Ce in each sample. As shown in Fig.4(C) and (D), CeO_2@MMT and free CeO_2 had Ce^{3+} ratios of 50.59% and 40.97%, respectively. The higher Ce^{3+} ratio in CeO_2@MMT may be attributed to the heterogeneous nucleation of MMT, which led to smaller CeO_2 particle sizes. Generally, CeO_2 NPs with smaller particle sizes have larger specific surface areas and more oxygen vacancies, resulting in more effective ROS scavenging[25].

3.2 ROS Scavenging Activity of CeO_2@MMT

Studies have shown that excessive ROS plays an important role in the pathogenesis of IBD[11,12]. Therefore, we selected $^{\cdot}O_2^-$ and H_2O_2, two typical ROS involved in the development of IBD, to study the ROS scavenging activity of CeO_2@MMT.

An oxygen electrode was used to detect the amount of O_2 produced by catalytic decomposition of H_2O_2 in 10 min, and the O_2 generation directly reflected the CAT-like activity of the materials[26]. As shown in Fig.5(A), compared with CeO_2, the amount of O_2 generated by CeO_2@MMT(containing the same content of CeO_2) was much higher. A concentration-dependent CAT-like activity was observed for both CeO_2 and

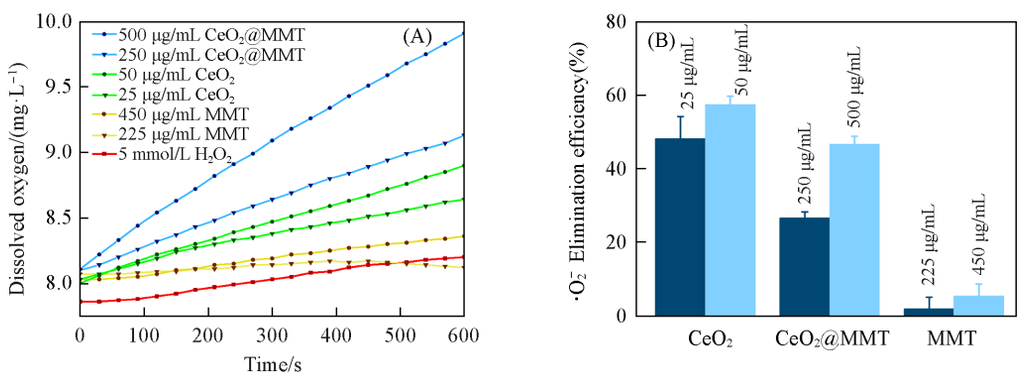

Fig. 5 ROS scavenging activity of CeO_2@MMT

(A) CAT-like activity test. Typical kinetic curves of oxygen generation from the decomposition of H_2O_2 in the presence of indicated materials recorded every 30 s for 10 min. (B) SOD-like activity and $^{\cdot}O_2^-$ scavenging rates of indicated materials. Data are presented as mean±standard error of the mean(n=4).

CeO_2@MMT. For example, under the catalysis of CeO_2@MMT, O_2 generated was 1.03 mg/L (containing 25 μg/mL CeO_2) and 1.8 mg/L (containing 50 μg/mL CeO_2) in 10 min, respectively. In addition, MMT showed little CAT-like activity at different concentrations. The above results showed that CeO_2@MMT had excellent CAT-like activity *in vitro*.

The SOD-like activity of CeO_2@MMT was directly correlated with the amount of $^{\cdot}O_2^-$ it could eliminate, which was detected by a $^{\cdot}O_2^-$-specific WST-1 kit. As shown in Fig.5(B), CeO_2@MMT showed a slightly lower $^{\cdot}O_2^-$ elimination efficiency than CeO_2 (containing the same concentration of CeO_2). As expected, the same amount of MMT exhibited negligible $^{\cdot}O_2^-$ elimination activity. Therefore, these results showed that CeO_2@MMT had satisfactory SOD-like activity.

3.3 Cytotoxicity and Cellular ROS Scavenging Activity

After studying the ROS scavenging activity of CeO_2@MMT *in vitro*, we further carried out cellular experiments to detect its cytotoxicity and its ability to scavenge ROS in cells. We selected RAW264.7 macrophages, which are closely related to epithelial lesions of IBD.

First, we investigated the cytotoxicity of CeO_2@MMT. As shown in Fig.6(A), CeO_2 and MMT showed good biocompatibility with RAW264.7 cells. Even when the concentration of the two materials was as high as 50 and 100 μg/mL, respectively, there was no obvious cytotoxicity, which was consistent with the previous research[20]. CeO_2@MMT showed negligible cytotoxicity when the concentration was lower than 12.5 μg/mL, and slight and concentration-dependent cytotoxicity could be observed for high concentrations.

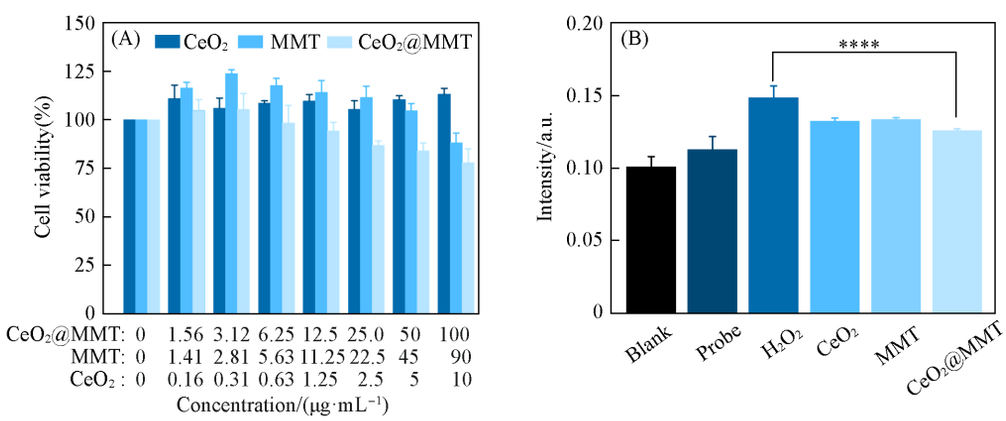

Fig. 6 Cell viability after incubation with indicated materials for 24 h(A) and ROS level of RAW264.7 macrophages pretreated with indicated materials under H_2O_2(100 μmol/L) stimulation(B)

Data are presented as mean±standard error of the mean(n=5). ****P < 0.0001 compared to the H_2O_2 group.

To verify whether CeO_2@MMT has the ability to protect cells from ROS-induced damage, we established an oxidative stress model of RAW264.7 cells stimulated with H_2O_2[Fig.6(B)]. First, the cells pretreated with the materials were stimulated with H_2O_2 and then incubated with the ROS-sensitive probe, DCFH-DA. After the incubation, the intracellular ROS level was detected and analyzed by a microplate reader. Compared with the H_2O_2-only stimulation group, treatment with CeO_2 obviously decreased the ROS level in RAW264.7 cells, with an elimination rate of approximately 45.6%, while the elimination rate of intracellular ROS by CeO_2@MMT was as high as 64.1%[Fig.6(B)]. The above results demonstrated that CeO_2@MMT exhibited satisfactory biocompatibility and cellular ROS scavenging activity.

3.4 Amelioration of CD with CeO_2@MMT

Encouraged by the good therapeutic effect of CeO_2@MMT in an ulcerative colitis model[20], we used a TNBS-induced CD mouse model (C57BL/6 strain) to investigate its universality in the treatment of IBD. We are aware that the TNBS-induced CD model could not capture all the pathological features in humans.

However, currently it is a suitable and well-recognized model for CD research[27,28]. At the same time, to explore the possibility of its clinical application, we compared its therapeutic efficacy *in vivo* with a clinical drug 5-ASA. On the first day, TNBS solution was absorbed through the skin to presensitize the mice. On the 8th day, TNBS solution was slowly injected into the colon cavity of mice to induce CD. CeO_2@MMT was then orally administered to mice once a day for three consecutive days after induction. The therapeutic efficacy of the materials was investigated by measuring the changes in body weight, colon length, and levels of pro-inflammatory cytokines and by analyzing the histologically stained colon sections(Fig.7).

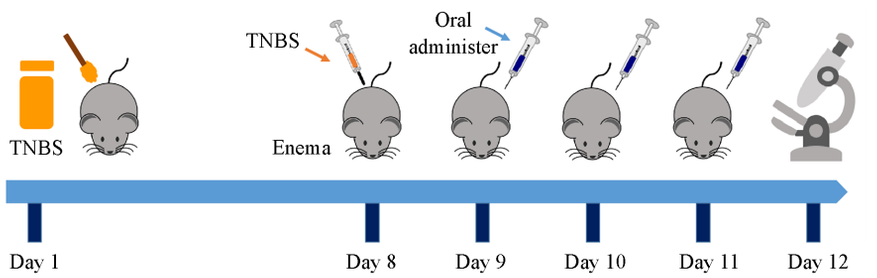

Fig. 7 Schematic diagram of the TNBS-induced CD model in mice and CeO_2@MMT treatment plan

On the first day, TNBS solution was absorbed through the skin to presensitize the mice. Control group mice were the healthy control group. Sham group mice were treated with saline enema on the ninth day. Saline, CeO_2, MMT, CeO_2@MMT, and 5-ASA mice were treated with TNBS enema on the ninth day and then administered saline, CeO_2, MMT, CeO_2@MMT, and 5-ASA at 1 mg/kg bodyweight once a day for three consecutive days.

Weight loss is a typical feature of mice with IBD. Therefore, weight monitoring can effectively reflect the successful establishment of the model and the therapeutic effect of drugs. As shown in Fig.8(A), on the second day of TNBS enema induction, all mice in the TNBS enema group showed obvious weight loss, while the weights of the healthy control group(Control) and saline enema group(Sham) remained stable. After three days of treatment, the weight of mice treated with CeO_2@MMT increased significantly, and the weight-loss trend of mice treated with 5-ASA and CeO_2 slightly improved. Meanwhile, the weight of the mice treated with

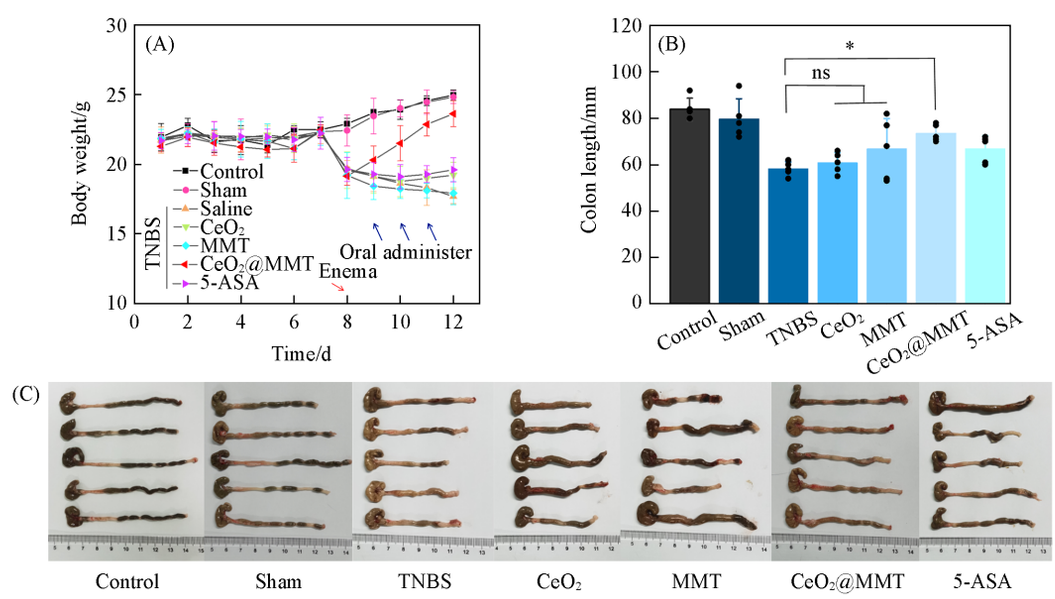

Fig. 8 Weight change and colon length statistics of different groups of mice

(A) The curves of weight changes of mice in different treatment groups; statistics(B) and photos(C) of colon length of mice in different treatment groups on day 12. Data are presented as mean±standard error of the mean(n=5). *P < 0.05 compared to the TNBS group.

MMT decreased.

Colon length shortening is another characteristic of mice with CD. Hence, colon length is another index that can effectively reflect the efficacy of drugs in addition to body weight. After three consecutive days of treatment, all the mice were euthanized on the 12th day, and the colon tissues of the mice were collected for measurement. As shown in Fig.8(B) and (C), the colon lengths of the five groups of mice induced by TNBS were all shorter than those of the healthy control group. In these five groups of mice, the groups treated with CeO_2@MMT and 5-ASA had an obvious protective effect on colon shortening, while that treated with CeO_2@MMT was even better.

The above results examined the therapeutic effect of materials on CD mice from a macroscopic point of view. To further verify its therapeutic effect, we studied organ tissue sections and levels of inflammatory factors in colon tissue.

As the representative slices of the colon of each experimental group shown in Fig.9, the colon tissues of Control group and Sham group kept normal tissue and cell morphology, with no detachment or loss of intestinal mucosa. However, in the saline group, there was a certain degree of shedding and loss of intestinal mucosa, which indicated that the CD model was successfully established. CeO_2 alleviated the tissue destruction in IBD to a certain extent, but the infiltration of inflammatory cells still existed, indicating that inflammation still existed. MMT also had a certain therapeutic effect on CD but failed to avoid colonic wall thickening. CeO_2@MMT and 5-ASA had good therapeutic effects on CD, maintaining good intestinal mucosa morphology and adhesion, avoiding thickening and edema of the intestinal wall, and relieving the degree of inflammation.

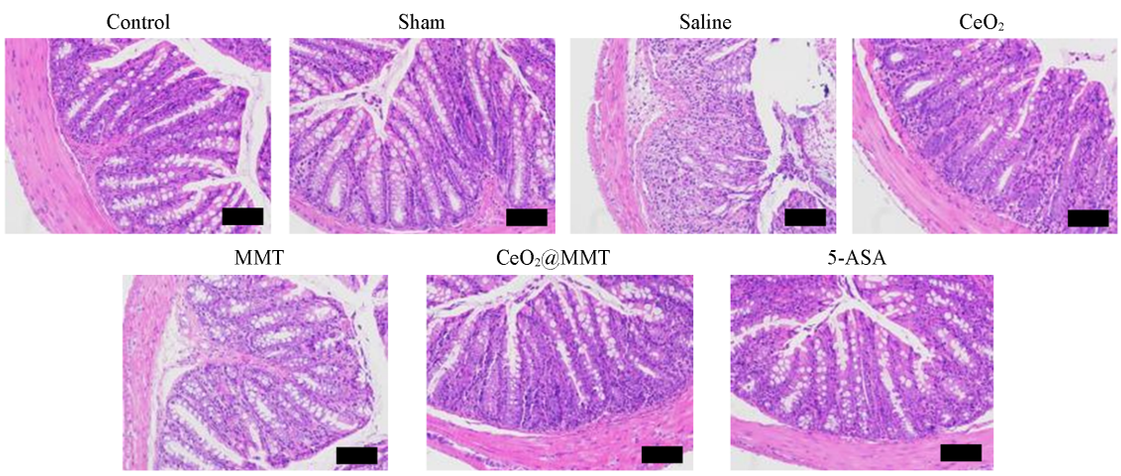

Fig. 9 Colon pathological sections(H&E staining) of different groups of mice on the 11th day

Scale bar: 100 μm.

As shown in Fig.10(A) and (B), enzyme linked immunosorbent assay(ELISA) showed that compared with the other treatment groups, the levels of IL-1β and TNF-α(typical pro-inflammatory factors) in the colon tissue of mice treated with CeO_2@MMT significantly decreased, which proved that CeO_2@MMT played an excellent anti-inflammatory role in the treatment of CD.

In terms of biological safety, we evaluated the hematoxylin-eosin(H&E)-stained sections of the major organs of mice in each experimental group for 7 d[Fig.11(A)] and 30 d[Fig.11(B)] after administration. Pathological results of the heart, liver, spleen, lung, and kidney in each experimental group showed no significant difference from those in the control group. At the dosage given in this study, none of the materials caused significant damage or pathological changes to the main organs of mice. The above experimental results

verified the good biological safety of the materials in this study.

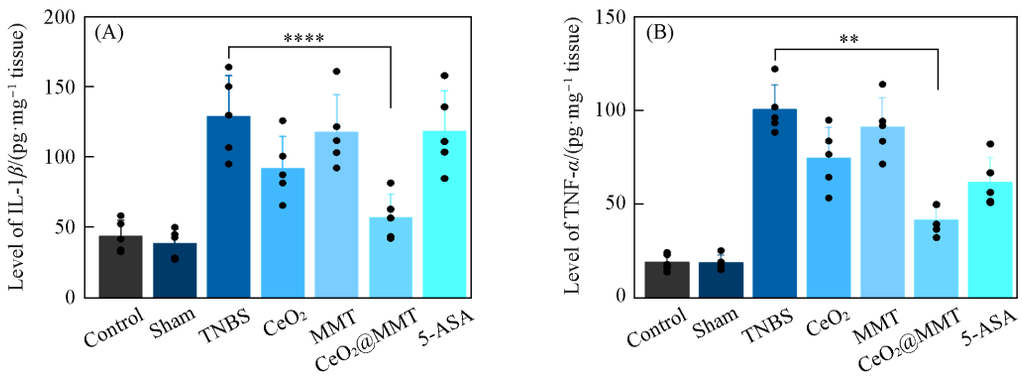

Fig. 10 Local concentrations of the proinflammatory cytokines IL-1β(A) and TNF-α(B) in colon homogenate of different groups of mice on the 12th day

Data are presented as mean±standard error of the mean (n = 5). **** P < 0.0001 and ** P < 0.01, comparison between TNBS group and CeO_2@MMT group.

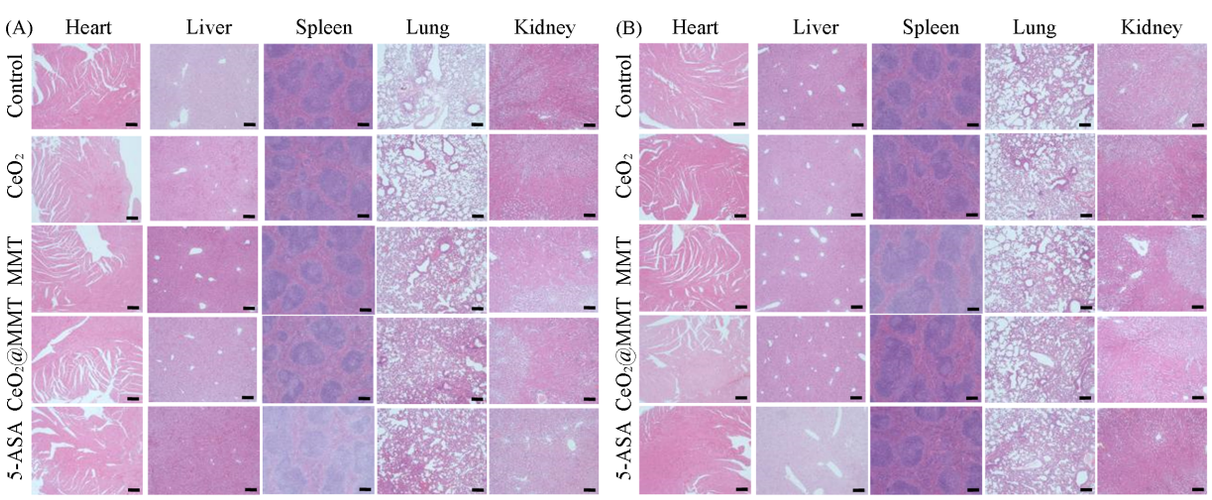

Fig. 11 Pathological sections(H&E staining) of the heart, liver, spleen, lung, and kidney of different groups of mice after 7 d(A) and 30 d(B) of administration

Scale bar: 200 μm.

4 Conclusions

CeO_2@MMT, which was designed and synthesized by our research group in the early stage, was used to expand its therapeutic effect on CD through *in vitro* and *in vivo* experiments. In the current study, TEM, SEM, *zeta* potential and other characterization confirmed that we successfully prepared CeO_2@MMT nanozymes with good dispersibility, structural stability and inflammation site targeting capacity. Two typical ROS, $^{\cdot}O_2^-$ and H_2O_2, in the pathogenesis of IBD, were selected as substrates for the study of the ROS elimination activity of materials *in vitro*. The results showed that CeO_2@MMT exhibited satisfactory scavenging activity towards $^{\cdot}O_2^-$ and H_2O_2. Then, we established a CD mouse model induced by TNBS to evaluate the therapeutic effect of the materials *in vivo*. Together, results of body weight, colon length, and other indicators showed that CeO_2@MMT had an excellent therapeutic effect. Colon homogenate cytokine test results and H&E staining of organ tissue sections confirmed the protective effect of CeO_2@MMT on intestinal inflammatory sites from a microscopic perspective. Compared with the clinical drug 5-ASA, CeO_2@MMT showed an even

better therapeutic effect. In addition, at the dosage of this study, none of the materials in each group caused significant damage or pathological changes to the main organs of mice. Therefore, the CeO_2@MMT in this work has a good therapeutic effect, universality and application prospects in the treatment of IBD.

References

[1] Torres J., Mehandru S., Colombel J. F., Peyrin-Biroulet L., *Lancet*, **2017**, *389*, 1741—1755
[2] Ungaro R., Mehandru S., Allen P. B., Peyrin-Biroulet L., Colombel J. F., *Lancet*, **2017**, *389*, 1756—1770
[3] Kaplan G. G., *Nat. Rev. Gastroenterol. Hepatol.*, **2015**, *12*, 720—727
[4] Nagao-Kitamoto H., Kitamoto S., Kamada N., *Cancer Metastasis Rev.*, **2022**, 1—16
[5] Bernstein C. N., Fried M., Krabshuis J. H., Cohen H ., Eliakim R., Fedail S., Gearry R., Goh K. L., Hamid S., Khan A. G ., LeMair A. W., Malfertheiner, Qin O., Rey J. F., Sood A., Steinwurz F., Thomsen O. O., Thomson A., Watermeyer G., *Inflamm. Bowel Dis.*, **2010**, *16*, 112—124
[6] Wilson D. S., Dalmasso G., Wang L., Sitaraman S. V., Merlin D., Murthy N., *Nat. Mater.*, **2010**, *9*, 923—928
[7] Chapkin R. S., Kamen B. A., Callaway E. S., Davidson L. A., George N. I., Wang N., Lupton J. R., Finnell R. H., *J. Nutr. Biochem.*, **2009**, *20*, 649—655
[8] Lautenschlager C., Schmidt C., Fischer D., Stallmach A., *Adv. Drug Deliv. Rev.*, **2014**, *71*, 58—76
[9] Farkas S., Hornung M., Sattler C., Anthuber M., Gunthert U., Herfarth H., Schlitt H. J., Geissler E. K., Wittig B. M., *Clin. Exp. Immunol.*, **2005**, *142*, 260—267
[10] Zhang S., Ermann J., Succi M. D., Zhou A., Hamilton M. J., Cao B., Korzenik J. R., Glickman J. N., Vemula P. K., Glimcher L. H., Traverso G., Langer R., Karp J. M., *Sci. Transl. Med.*, **2015**, *7*, 300ra128
[11] Roessner A., Kuester D., Malfertheiner P., Schneider S., *Pathol. Res. Pract.*, **2008**, *204*, 511—524
[12] Poli G., *Free Radic. Biol. Med.*, **2002**, *33*, 301—302
[13] Zhang Q., Tao H., Lin Y., Hu Y., An H., Zhang D., Feng S., Hu H., Wang R., Li X., Zhang J., *Biomaterials*, **2016**, *105*, 206—221
[14] Wei H., Wang E., *Chem. Soc. Rev.*, **2013**, *42*, 6060—6093
[15] Bao X., Zhao J., Sun J., Hu M., Yang X., *ACS Nano*, **2018**, *12*, 8882—8892
[16] Li S., Shang L., Xu B., Wang S., Gu K., Wu Q., Sun Y., Zhang Q., Yang H., Zhang F., Gu L., Zhang T., Liu H., *Angew. Chem. Int. Ed.*, **2019**, *58*, 12624—12631
[17] Li Y., He X., Yin J., Ma Y., Zhang P., Li J., Ding Y., Zhang J., Zhao Y., Chai Z., Zhang Z., *Angew. Chem. Int. Ed.*, **2015**, *54*, 1832—1835
[18] Xi J., Zhang R., Wang L., Xu W., Liang Q., Li J., Jiang J., Yang Y., Yan X., Fan K., Gao L., *Adv. Funct. Mater.*, **2021**, *31*, 2007130
[19] Zhang Y., Wang F., Liu C., Wang Z., Kang L., Huang Y., Dong K., Ren J., Qu X., *ACS Nano*, **2018**, *12*, 651—661
[20] Zhao S., Li Y., Liu Q., Li S., Cheng Y., Cheng C., Sun Z., Du Y., Butch C. J., Wei H., *Adv. Funct. Mater.*, **2020**, *30*, 2004692—2004706
[21] Korsvik C., Patil S., Seal S., Self W. T., *Chem. Commun.(Camb.)*, **2007**, *10*, 1056—1058
[22] Reed K., Cormack A., Kulkarni A., Mayton M., Sayle D., Klaessig F., Stadler B., *ChemInform*, **2015**, *46*, 390—405
[23] Ivanov V. K., Shcherbakov A. B., Usatenko A. V., *Russ. Chem. Rev.*, **2009**, *78*, 855—871
[24] Heckert E. G., Karakoti A. S., Seal S., Self W. T., *Biomaterials*, **2008**, *29*, 2705—2709
[25] Deshpande S., Patil S., Kuchibhatla S. V. N. T., Seal S., *Appl. Phys. Lett.*, **2005**, *87*, 3113—3115
[26] Liu Y., Cheng Y., Zhang H., Zhou M., Yu Y., Lin S., Jiang B., Zhao X., Miao L., Wei C., Liu Q., Lin Y., Du Y., Butch C. J., Wei H., *Sci. Adv.*, **2020**, *6*, eabb2695
[27] Wirtz S., Popp V., Kindermann M., Gerlach K., Weigmann B., Fichtner-Feigl S., Neurath M. F., *Nat. Protoc.*, **2017**, *12*, 1295
[28] Neurath M., Fuss I., Strober W. *Int. Rev. Immunol.*, **2000**, *19*, 51—62

(Ed.: W, K, M)